IEEE Open Journal of Engineering in Medicine and Biology

Technology

Information-Theoretic Analysis of EEG Wave Amplitude and Heart Rate Variability Reveals the Time Scale-Dependent Nature of Brain-Heart Interactions

Valeria Rosalia Vergara, Chiara Barà, *Student Member, IEEE*, Andrea Zaccaro, Francesca Ferri, Fabrice Jurysta, Luca Faes, *Senior Member, IEEE*, and Yuri Antonacci, *Member, IEEE*

***Abstract*—*Goal*: Brain-heart interactions have been linked to physiological and pathological states and are typically studied through the use of electroencephalographic (EEG) signal and heart rate variability (HRV) time series. However, there are still major challenges to overcome, particularly in establishing a robust methodology to assess these complex multi-scale interactions and to extract meaningful information. To this end, we explore the time scale-dependent nature of brain-heart interactions by exploiting information-theoretic measures. *Methods*: We analyze cardiac vagal activity and EEG brain wave amplitudes at two time scales —heart rhythm (∼1s) and longer (∼1min)—in two groups of healthy subjects respectively monitored during wakefulness and sleep, respectively. Different entropy-based measures are then employed to evaluate the regularity of each system's dynamics as well as their static and dynamic coupling. *Results*: Different time-scales are involved in different physiological coupling mechanisms. While overall coupling strength values are low, longer time-scales show a stronger presence of coupling in terms of statistically validated brain-heart connections compared to shorter time-scales. *Conclusions*: This study shows that the presence and the strength of brain-heart interactions are highly dependent on the time-scale, which in turn is affected by the underlying physiological processes.**

***Index Terms*—Brain-Heart axis, EEG, Heart Rate Variability, Information Theory, Network Physiology**

***Impact Statement*- Within the framework of information theory, this study enhances the understanding of brain-heart interplay by showing how its strength and dynamics depend on the time-scale of observation.**

I. INTRODUCTION

THE study of brain-heart interactions has gained significant attention due to their crucial role in sustaining human physiological regulation [1]. Several studies have linked alterations in brain-heart communication to cardiovascular, neurological, and psychiatric disorders [2]. Since brain and cardiac systems operate across multiple time scales [3], their complex fluctuations necessitate nonlinear analytical approaches to accurately capture the intricate dynamics [4].

Several studies rely on non-invasive measures of brain and heart activities, particularly electroencephalography (EEG) and electrocardiography (ECG), which are well-suited to investigate the rapid dynamics of both physiological systems [5]. Key methods for exploring the interplay between cardiac activity and cortical processes include the heartbeat-evoked potential [6] and the correlation between ECG-derived heart rate variability (HRV) and the spectral dynamics of EEG oscillations. These analyses are conducted at the cardiac cycle time-scale (∼1 second) to capture heartbeat-related responses across various physiopathological conditions [7]–[11], as well as at longer time-scales (∼1 minute) to examine broader oscillatory dynamics [12], [13]. While a wide range of methodological approaches have been developed for investigating EEG-HRV brain-heart interactions [11], [14], [15], information-theoretic measures have emerged as particularly promising [9], [12], [13], [16], [17] due to their ability to capture complex behaviors without assumptions about data distributions or reliance on discretization procedures that could bias estimates [18].

Entropy-based measures like Information Storage (IS) [19], Mutual Information (MI) [20] and Mutual Information Rate (MIR) [21] have been applied to study different aspects of brain-heart dynamics in a variety of contexts, including wakefulness and sleep [13], stress and rest [22], [23], mental workload and relaxation [24], as well as emotional arousal and neutral states [25], as they enable the quantification of information stored within and exchanged between the brain and heart systems. Despite these methodological advances, a unified framework capable of comprehensively capturing the complexity of brain-heart dynamics is still lacking. Moreover, the wide variety of methods and their dependence on specific physiological states, which characterize different temporal dynamics, often lead to divergent results [17].

This work was supported by SiciliAn MicronanOTecH Research And Innovation CEnter "SAMOTHRACE" (MUR, PNRR-M4C2, ECS_00000022), spoke 3 - Università degli Studi di Palermo "S2-COMMs - Micro and Nanotechnologies for Smart & Sustainable Communities and by PRIN 2022 project "HONEST-High-Order Dynamical Networks in Computational Neuroscience and Physiology: an Information-Theoretic Framework" (funded by MUR, code 2022YMHNPY, CUP B53D23003020006);

Valeria R. Vergara, L. Faes, C. Barà and Y. Antonacci are with the Department of Engineering, University of Palermo, Palermo, Italy (correspondence e-mail: yuri.antonacci@unipa.it). A. Zaccaro and F. Ferri are with the Department of Neuroscience, Imaging and Clinical Sciences, "G. d'Annunzio" University of Chieti-Pescara, Chieti, Italy. F. Ferri is with Institute for Advanced Biomedical Technologies (ITAB), "G. d'Annunzio" University of Chieti-Pescara, Chieti, Italy. F. Jurysta is with Doctor Fabrice Jurysta Medical Centers, Brussels, Belgium

This study aims to provide a comprehensive analysis of brain-heart interactions, emphasizing how the time-scales at which EEG and HRV series are built influence both the coupling between the two systems and the internal dynamics of each system. Specifically, we compare the effects of the aforementioned time-scales to investigate brain-heart interactions: a shorter time-scale ($\sim$ 1s), corresponding to heart rhythms during wakefulness, and a longer time-scale ($\sim$ 1min), representative of sleep dynamics. IS is applied to characterize the complexity and predictability of brain and heart dynamics, while the strength of bidirectional static and dynamic coupling is assessed using MI and MIR, respectively [26]. The analysis aims to show whether and how the regular dynamics of HRV and EEG amplitude, as well as their coupling, are peculiar of the considered time-scale and physiological condition.

II. MATERIALS AND METHODS

A. Datasets description and time-series extraction

Dataset 1: The dataset comprises resting state EEG and ECG signals from eighteen healthy subjects (14 females; age: 28.28 $\pm$ 4.78 years). EEG was acquired using a 64-channel BrainAmp (Brain Vision) amplifier (10/20 system, $f_s = 2k$Hz; FC_z reference) [27], and ECG signal with a one-lead system (BIOPAC System, INC, lead I, $f_s = 2k$Hz). Participants were asked to rest with their eyes open for about 10 minutes. For additional information about acquisition system and protocol see [27].

R-peaks of the ECG signal were detected using the Pan-Tompkins algorithm, and the time intervals between two consecutive R-peaks in the ECG trace were measured (Fig.1a). Outliers (samples exceeding three standard deviations from the mean) were removed and the resulting gaps were interpolated to obtain 300 RR intervals. Two additional cardiac time series were computed [28]: SD_{RR}, as the first-order differences of RR intervals ($RR_{i+1} - RR_i$ for $i = 1, \ldots, 299$), and P_{RR-HF} (Fig.1b), extracted from the time-resolved spectrogram of RR intervals. The spectrogram was generated using a high-pass AR filter (zero phase, cut-off frequency 0.0185 Hz) followed by the smoothed pseudo-Wigner-Ville distribution [29]. It was then integrated over the range [0.15–0.4] Hz and normalized to the total power in [0.04–0.4] Hz.

Brain signals were firstly bandpass-filtered (0.5–40 Hz) and the ocular artifacts removed via ICA (fastICA algorithm), down-sampled to 128 Hz, and re-referenced to the average [27] (Matlab 21.1 (MathWorks Inc.) -EEGLAB Toolbox [30]). EEG time series were segmented by cardiac cycles [13] (Fig.1a) and the power spectral density (PSD) of each channel and segment was estimated using the weighted covariance method (Hamming window, $\tau = 64$, no overlapping) [31]. Brain wave power was averaged within δ ([2–4] Hz), θ ([4–8] Hz), α ([8–13] Hz), and β ([13–33] Hz) bands, with the total EEG power ($P_{EEG_{TOT}}$) derived from signal variance within each RR interval (Fig.1c). Four channels with electrode artifacts were excluded.

Overall, for each subject, five brain time series ($P_{EEG_{TOT}}$, $P_{EEG\delta}$, $P_{EEG\theta}$, $P_{EEG\alpha}$, and $P_{EEG\beta}$) synchronous with the cardiac time series (RR, SD_{RR}, and P_{RR-HF}) were obtained.

Dataset 2: The dataset comprises EEG (Fz-Ax, Cz-Ax, Oz-Ax; Ax mastoid reference, f_s =100 Hz) and ECG (lead II, f_s =200 Hz) recordings from ten male volunteers (ages 18-23) monitored overnight using a digital polygraph (Brainnet, Medatec, Brussels). Brain and cardiac signals were pre-processed to generate synchronous time-series at a time-scale of approximately 1 minute.

QRS complexes were detected automatically and RR interval time series derived following a validated procedure [32]. After correcting for artifacts and ectopic beats, RR intervals were interpolated, resampled at 8 Hz, and subdivided in consecutive windows of 120 s overlapped by half. For each window RR series were detrended, Hanning windowed, and fast Fourier transformed to obtain the relevant power spectral density. Finally, the time series representing cardiac parasympathetic activity was derived by normalizing the spectral power in the HF band [0.15–0.4] Hz to the total power within the [0.04–0.4] Hz range [32], [33].

EEG signals were analyzed to extract five brain wave amplitude time series. Spectral power was computed via fast Fourier transform applied to consecutive 5-second windows of the Cz-Ax channel, focusing on conventional sleep-related frequency bands [13], [32] (δ: [0.5–3 Hz]; θ: [3–8 Hz]; α: [8–12 Hz]; σ: [12–16 Hz]; β: [16–25 Hz]). Brain wave amplitudes (Fig.2a) were computed as the ratio between the spectral power within each frequency band and its average across the entire night, following the approach described in [34], and were then averaged over 60-second intervals. The fast Fourier transformations were performed via MATLAB (The Math Works Inc., USA) and its signal processing toolbox (v 5.1, Fig.2a).

Six synchronized time series were obtained at 60-seconds resolution during the whole-night, irrespective of sleep stages, for each subject (P_{RR-HF}, $P_{EEG\delta}$, $P_{EEG\theta}$, $P_{EEG\alpha}$, $P_{EEG\sigma}$, and $P_{EEG\beta}$), with lengths varying between 460 and 500 samples (N: 464.60 $\pm$ 34.26). Time series for a representative subject are shown in Fig.2b. A detailed description of the polysomnography protocol and time series measurement is available in [32].

B. Information Domain Analysis

Cardiac and brain time series were modeled as realizations of a stationary and ergodic bivariate process $S = [X, Y]$, where X and Y represent heart and brain activity, respectively. Assuming S is a Markov process of order m, X_n and Y_n denote the present states of the processes, while $X_n^m = [X_{n-1}, \ldots, X_{n-m}]$ and $Y_n^m = [Y_{n-1}, \ldots, Y_{n-m}]$ their past states. IS, MI, and MIR were estimated using the k-Nearest-Neighbors approach [13], [35], which capture nonlinear dynamics without assumptions about probability distributions, minimizing bias in entropy computation for variables of differing dimensions [35].

1) Information Storage: IS quantifies the information contained in the past of a process that can be used to predict its future measuring the average uncertainty about the present state

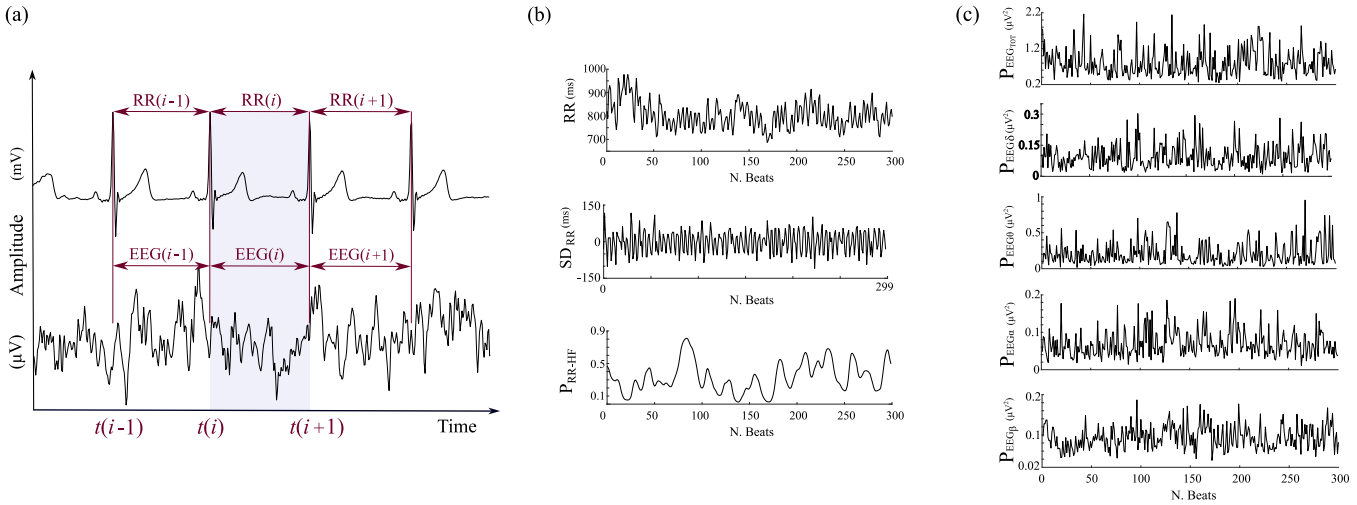

Fig. 1. (**a**) Example of ECG (top) and one-channel EEG (bottom) signals of one representative subject during wakefulness [27]. A shorter time-scale is considered for the time series extraction process, specifically the cardiac cycle ($\sim$ 1s), defined as the time interval between two consecutive ECG R-peaks. (**b**) Example of the time series representative of the cardiac activity, i.e., the RR intervals (*RR*), the successive difference of consecutive RR intervals (SD_{RR}), and the normalized HF power of the RR intervals (P_{RR-HF}). (**c**) Example of the time series representative of brain dynamics, i.e., the total power ($P_{EEG_{TOT}}$) and the power of spectral band components δ ($P_{EEG\delta}$), θ ($P_{EEG\theta}$), α ($P_{EEG\alpha}$) and β ($P_{EEG\beta}$).

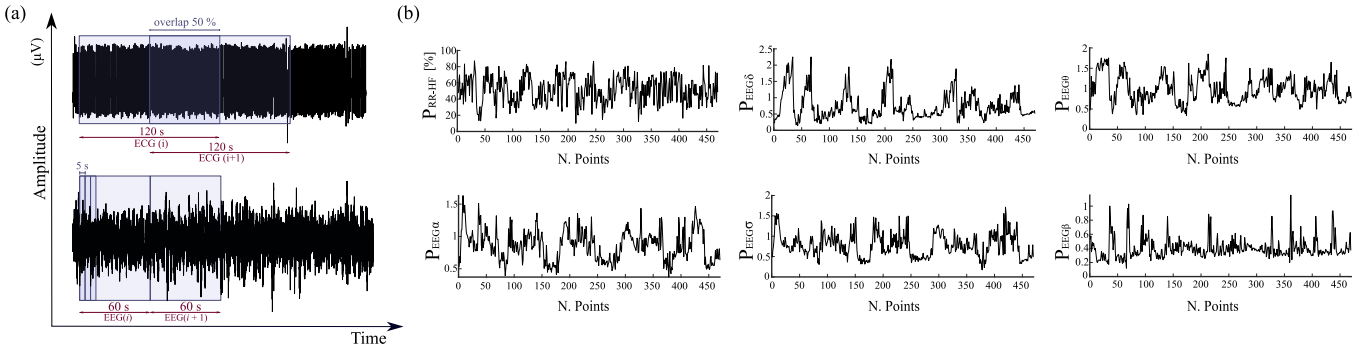

Fig. 2. (**a**) Example of ECG (top) and EEG (bottom) signals of one representative subject during sleep [32]. A 120 s window overlapped by half and a 60 s window were identified on RR series and EEG signal, respectively, for obtaining each spectral components. (**b**) Example of brain and heart time series synchronously measured at a longer time-scale, i.e., every 60 s, during whole-night polysomnography, quantifying the evolution over time of the normalized HF power of the RR intervals (P_{RR-HF}, expressed as a percentage) and of the normalized EEG power within the δ ($P_{EEG\delta}$), θ ($P_{EEG\theta}$), α ($P_{EEG\alpha}$), σ ($P_{EEG\sigma}$), and β ($P_{EEG\beta}$) frequency bands. Note that for the brain time-series, values greater than 1 reflect time periods in which the power exceeds the whole-night mean.

of the process that is resolved when its past states are known [19]. For a process X, IS is as:

$$S_X = I(X_n; X_n^m) = H(X_n) - H(X_n|X_n^m), \tag{1}$$

where $I(\cdot;\cdot)$ is MI between two random variables, and $H(\cdot)$ and $H(\cdot|\cdot)$ denote entropy and conditional entropy (CE), respectively. Estimating IS involves decomposing CE into joint entropy terms [36], [37]:

$$S_X = H(X_n) + H(X_n^m) - H(X_n, X_n^m). \tag{2}$$

The first step of the KSG estimation approach involves calculating the entropy term in the highest-dimensional space and determining sample distances using the maximum norm:

$$H(X_n, X_n^m) = -\psi(k) + \psi(N) + (m+1)\langle log\varepsilon_{n,k}\rangle, \tag{3}$$

where $\psi(\cdot)$ is the digamma function, N is the total number of available $(m+1)$-dimensional points $[X_n, X_n^m]$, $\varepsilon_{n,k}$ is twice the distance from $[X_n, X_n^m]$ to its k-th neighbor, and $\langle\cdot\rangle$ denotes average over all samples. The obtained searching distances were used to perform range searches in lower-dimensional projected subspaces [20]. The other two entropy terms presented in Eq. (2) are obtained as follows:

$$H(X_n) = \psi(N) - \langle\psi(N_{X_n} + 1)\rangle + \langle log\varepsilon_{n,k}\rangle, \tag{4}$$

$$H(X_n^m) = \psi(N) - \langle\psi(N_{X_n^m} + 1)\rangle + m\langle log\varepsilon_{n,k}\rangle, \tag{5}$$

where N_{X_n} and $N_{X_n^m}$ are number of points whose distance from X_n and X_n^m, respectively, is strictly less than $\varepsilon_{n,k}/2$. Then, an estimate of S_X is obtained by substituting (3), (4) and (5) into

(2):

$$IS = \psi(k) + \psi(N) - \langle \psi(N_{X_n} + 1) + \psi(N_{X_n^m} + 1) \rangle. \quad (6)$$

The same holds for process Y representing each EEG power time series (S_Y).

2) Mutual Information: MI quantifies the information shared by two systems at each moment in time by measuring the average uncertainty about the current state of X that is resolved by knowing the present state of Y [36]:

$$I(X_n;Y_n) = H(X_n) + H(Y_n) - H(X_n,Y_n). \quad (7)$$

MI is obtained by searching for neighbors in the high-dimensional space $[X_n,Y_n]$ and performing range searches in its lower-dimensional projections. The KSG formulations facilitate the estimation of all entropy terms in Eq. (7) as follows:

$$H(X_n,Y_n) = -\psi(k) + \psi(N) + 2\langle log\varepsilon_{n,k} \rangle, \quad (8)$$

$$H(X_n) = \psi(N) - \langle \psi(N_{X_n} + 1) \rangle + \langle log\varepsilon_{n,k} \rangle, \quad (9)$$

$$H(Y_n) = \psi(N) - \langle \psi(N_{Y_n} + 1) \rangle + \langle log\varepsilon_{n,k} \rangle, \quad (10)$$

where N is the total number of available bi-dimensional samples $[X_n,Y_n]$, $\varepsilon_{n,k}$ is twice the distance from $[X_n,Y_n]$ to its k-th neighbor, and N_{X_n} and N_{Y_n} are the number of points whose distance from X_n and Y_n is strictly less than $\varepsilon_{n,k}/2$.

Substituting the terms obtained in Eqs.(8), (9) and (10) into (7), an estimate of the MI is obtained as follows:

$$MI = \psi(k) + \psi(N) - \langle \psi(N_{X_n} + 1) + \psi(N_{Y_n} + 1) \rangle. \quad (11)$$

3) Mutual Information Rate: MIR quantifies the information shared per unit of time [26], [37] between X and Y and can be defined as [38]:

$$I_{X;Y} = H(X_n|X_n^m) + H(Y_n|Y_n^m) - H(X_n,Y_n|X_n^m,Y_n^m). \quad (12)$$

Estimating MIR requires six entropy terms, as each CE term is the difference between two entropies. These terms can be estimated using the KSG formulation as follows [21]:

$$H(X_n,Y_n,X_n^m,Y_n^m) = -\psi(k) + \psi(N) + 2(m+1)\langle log\varepsilon_{n,k} \rangle, \quad (13)$$

$$H(X_n^m,Y_n^m) = \psi(N) - \langle \psi(N_{X_n^m,Y_n^m} + 1) \rangle + 2m\langle log\varepsilon_{n,k} \rangle, \quad (14)$$

$$H(X_n,X_n^m) = \psi(N) - \langle \psi(N_{X_n,X_n^m} + 1) \rangle + (m+1)\langle log\varepsilon_{n,k} \rangle, \quad (15)$$

$$H(Y_n,Y_n^m) = \psi(N) - \langle \psi(N_{Y_n,Y_n^m} + 1) \rangle + (m+1)\langle log\varepsilon_{n,k} \rangle, \quad (16)$$

$$H(X_n^m) = \psi(N) - \langle \psi(N_{X_n^m} + 1) \rangle + m\langle log\varepsilon_{n,k} \rangle, \quad (17)$$

$$H(Y_n^m) = \psi(N) - \langle \psi(N_{Y_n^m} + 1) \rangle + m\langle log\varepsilon_{n,k} \rangle, \quad (18)$$

where N is the total number of available $2(m+1)$-dimensional points $[X_n,Y_n,X_n^m,Y_n^m]$, and $N_{X_n^m,Y_n^m}$, N_{X_n,X_n^m}, N_{Y_n,Y_n^m}, N_{X_n} and N_{Y_n} are the number of points whose distance from the correspondent reference points is smaller than $\varepsilon_{n,k}/2$ in the lower dimensional spaces (i.e., $[X_n^m,Y_n^m]$, $[X_n,X_n^m]$, $[Y_n,Y_n^m]$, X_n and Y_n, respectively), being $\varepsilon_{n,k}$ twice the distance from samples in $[X_n,Y_n,X_n^m,Y_n^m]$ to the k-th neighbors. Thus, an estimate of MIR can be obtained as:

$$\begin{aligned} MIR = \psi(k) + \langle & \psi(N_{X_n^m} + 1) + \psi(N_{Y_n^m} + 1) \\ & - \psi(N_{X_n,X_n^m} + 1) - \psi(N_{Y_n,Y_n^m} + 1) - \psi(N_{x_n^m,Y_n^m} + 1) \rangle. \end{aligned} \quad (19)$$

C. Data and statistical analysis

Time series were normalized to zero-mean and unit variance and tested for stationarity in mean using the Mann-Whitney U-test [39]. Then, the information-theoretic measures of IS, MI, and MIR were computed on the time series extracted as described in Sect. II-A, to characterize heart and brain dynamics individually and their interactions across different time-scales. The computation of IS, MI and MIR was performed by exploiting ITS and MIR toolboxes (BITLab website) using Matlab 23.2. IS measure was computed for cardiac time series (Dataset-1: RR, SD_{RR}, and P_{RR-HF}; Dataset-2: P_{RR-HF}) and brain wave power time series (Dataset-1: P_{EEGb}, $b \in \{TOT,\delta,\theta,\alpha,\beta\}$; Dataset-2: P_{EEGb}, $b \in \{\delta,\theta,\alpha,\sigma,\beta\}$), while MI and MIR measures were computed to assess interactions between heart and brain activity, where the heart activities (Dataset-1: $X \in \{RR, SD_{RR}, P_{RR-HF}\}$; Dataset-2: $X = P_{RR-HF}$) was related to brain activity (Dataset-1: $Y = P_{EEGb}$, $b \in \{TOT,\delta,\theta,\alpha,\beta\}$; Dataset-2: $Y = P_{EEGb}$, $b \in \{\delta,\theta,\alpha,\sigma,\beta\}$). The searching neighbors was set to $k = 10$ and the past history dimension to $m = 2$ for IS and $m = 3$ for MIR, to mitigate the curse of dimensionality in model-free analyses [35]. For Dataset-1, measures were averaged across the entire scalp due to the observed quite uniform distribution. Modulation of IS, MI, and MIR across brain rhythms was assessed using a non-parametric paired Wilcoxon signed-rank test ($\alpha = 0.05$, Bonferroni correction, $n = 10$).

The significance of IS was assessed using a random shuffling [21] under the null hypothesis of no self-dependencies ($S_X = 0$). For MI and MIR, random time-shift surrogates were generated under the null hypothesis of independent heart and brain processes ($I(X_n;Y_n) = 0$, $I_{X;Y} = 0$) by shifting the cardiac time series forward with a minimum shift of 20 samples while keeping the brain series unchanged [40]. One hundred surrogates were generated for Dataset 1 and ten thousand for Dataset 2 to balance the higher computational cost of Dataset 1 with the need to minimize statistical fluctuations in Dataset 2. Statistical significance was evaluated using a nonparametric percentile-based test, considering a measure significant if it exceeded the $95th$ percentile of its surrogate distribution.

III. RESULTS

All time series used for the information domain analysis showed weak-sense stationarity of order one.

The IS analysis of the cardiac system (Table I) reveals a modulation of the regularity of the cardiac dynamics, with higher values at shorter time-scales ($\sim$ 1s), if compared to the longer one ($\sim$ 1min). Furthermore, surrogate data analysis confirms the presence of IS in 100% of subjects across all time-scales.

The boxplot distributions of IS across subjects (Fig.3) show that brain dynamics exhibit limited values of information stored at shorter time-scale ($\sim$ 1s, Fig.3*a*), but become significantly more predictable at longer time-scale ($\sim$ 1min, Fig.3*b*). While IS values increase with frequency of oscillations at shorter time-scale, an opposite trend emerges at longer time-scale, where δ oscillations exhibit the highest predictability. At both time-scales, information stored in δ brain waves is significantly

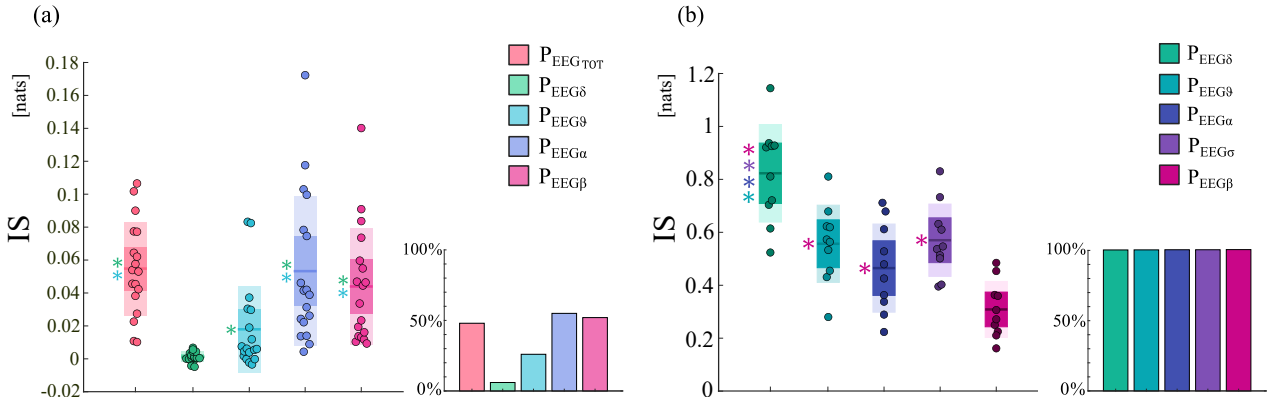

Fig. 3. Boxplots reporting the distributions and individual values of IS obtained for each EEG time series at shorter time-scale ($\sim$ 1s) during wakefulness (panel *a*) and at longer time-scale ($\sim$ 1min) during sleep (panel *b*); the bar plots in the bottom-right part of each panel represent the percentage of subjects for whom the presence of IS was deemed as statistically significant. Note that in the case of the shorter time-scale, both IS values and the percentage of IS values identified as statistically significant, according with surrogate data analysis, were firstly averaged across all EEG channels. Statistical test: $*$, $p < 0.05/10$, paired samples Wilcoxon test between pairs of brain rhythms, with Bonferroni correction.

TABLE I. IS values for the cardiac system derived from different time series extracted from the ECG signal at shorter (S) and longer (L) time-scales.

RR	SD_{RR}	P_{RR-HF}-S	P_{RR-HF}-L
0.61 $\pm$ 0.21	0.48 $\pm$ 0.17	1.63 $\pm$ 0.12	0.18 $\pm$ 0.05

different from that of other rhythms analyzed.

These findings are supported by surrogate data analysis, which shows statistically significant predictability in brain dynamics for only about 50% of subjects at shorter time-scale, with δ band exhibiting almost no statistically significant predictability. In contrast, at longer time-scale, statistically significant information content is observed in brain dynamics for 100% of subjects regardless of frequency bands.

The boxplot distributions of MI across subjects (Fig.4) denote a weak coupling between the brain and cardiac systems at shorter time-scales ($\sim$ 1s) regardless of the specific cardiac information extracted. In particular, only when the vagal component of the cardiac dynamics is considered (Fig.4*c*, P_{RR-HF}), the MI shows a statistically significant modulation in its strength across brain oscillations. These findings are further supported by surrogate data analysis, which shows statistically significant coupling in fewer than 10% of subjects across all brain rhythms, highlighting the absence of consistent brain-heart interactions at this time-scale.

Conversely, at the longer time-scale ($\sim$ 1min), although the strength of MI remains relatively low, the coupling between cardiac and brain dynamics becomes more prevalent, especially in the β frequency band. Indeed, surrogate data analysis reveals the presence of statistically significant coupling in 100% of subjects.

The boxplots illustrating the distributions of MIR across subjects (Fig.5) reveal weak levels of dynamic coupling between the cardiac and brain systems at both time-scales, consistent with the MI findings, although the MIR values are generally lower. Overall, the same observations noted for MI regarding frequency bands, cardiac metrics derived from RR intervals, and time-scales can be applied to the MIR measure. The main distinction is a higher level of presence in terms of statistically significant links observed at the longer time-scale ($\sim$ 1min) between the cardiac parasympathetic activity (P_{RR-HF}) and EEG brain waves (Fig.5 *d*). Specifically, MIR is statistically significant in approximately 80% of subjects for the δ, θ, α, and σ bands, and in 100% for the β band, while its presence is almost irrelevant at the shorter time-scale ($\sim$ 1s).

IV. DISCUSSION

A. Internal dynamics of cardiac and brain systems

The analysis of the HRV dynamics revealed higher strength values at shorter time-scales during wakefulness compared to longer time-scales during sleep. Surrogate data analysis confirmed the existence of predictability at both time-scales, potentially arising from fluctuations in autonomic activity that regulate the heart rhythm at rest [28] and during sleep [12], [41]. During non-REM stages, this regulation becomes more complex and variable, possibly explaining the reduced predictability of cardiac dynamics [13].

In contrast, brain dynamics exhibited scale-dependent behavior also in terms of significance. Shorter time-scales were characterized by higher regularity in α and β rhythms [8], [42], potentially reflecting default mode network activity during resting state [16], [42], [43]. However, surrogate data analysis indicated that the presence of these rhythms was not consistently significant across subjects, as shown in Fig.3 and previous studies [8] and can be related with the inter-subject variability of brain dynamics observed in previous work [44].

The low predictability in the δ band could be attributed to the temporal scale and filtering parameters of the data (i.e., the use of shorter time windows and the lower boundary of the δ frequency range lying close to the low cut-off frequency of the filter applied to the raw EEG).

At longer time-scales during sleep, increased IS values in

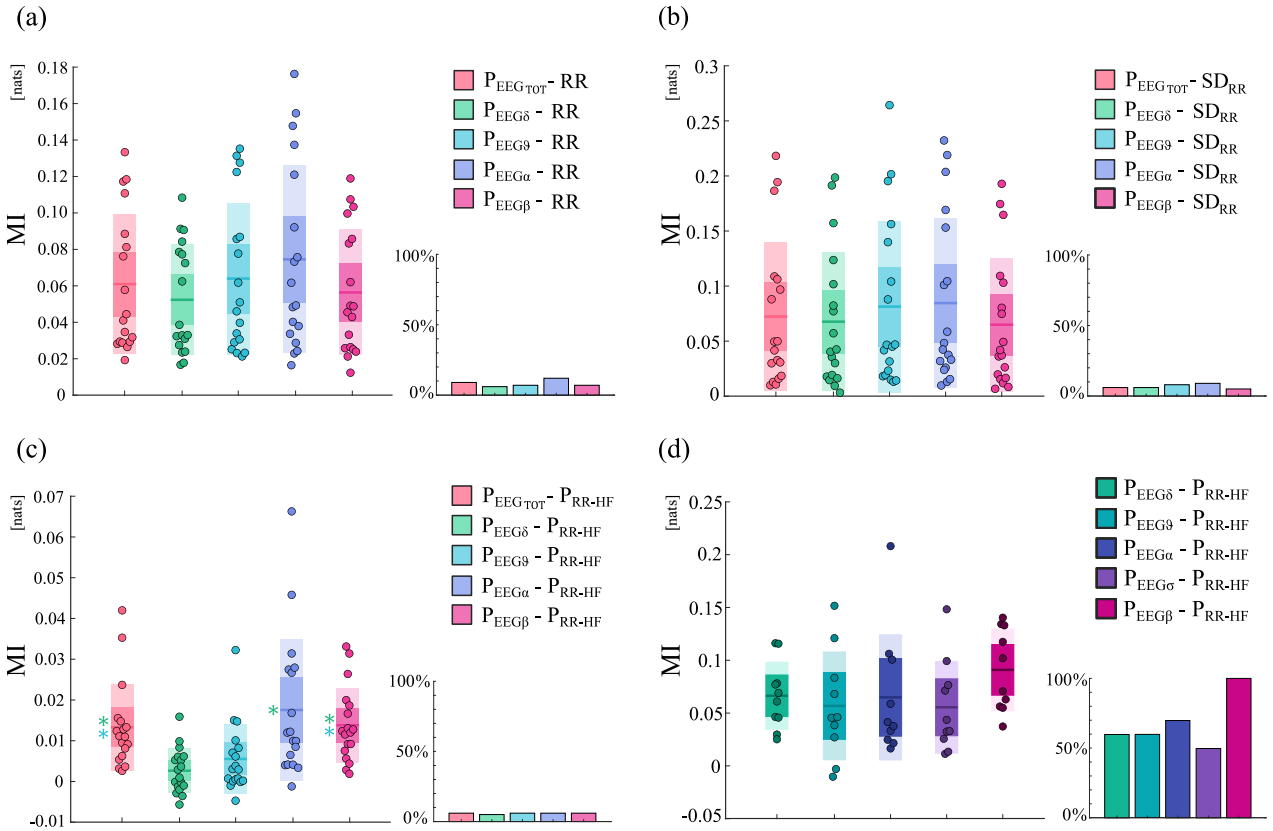

Fig. 4. Boxplots reporting the distributions and individual values of MI computed at shorter time-scale ($\sim$ 1s) during wakefulness (panels *a-c*) and at longer time-scale ($\sim$ 1min) during sleep (panel *d*) between the cardiac *RR*, SD_{RR}, P_{RR-HF} time series and each EEG time series; the bar plots in the bottom-right part of each panel represent the percentage of subjects for whom the presence of MI was deemed as statistically significant. For Dataset-1 (faster time-scale $\sim$ 1s) both MI values and the percentage of MI values identified as statistically significant, according with surrogate data analysis, were firstly averaged across all EEG channels. Statistical test: $*$, $p < 0.05/10$, paired samples Wilcoxon test between pairs of brain rhythms, with Bonferroni correction.

brain dynamics may be related to previously documented sleep-related EEG wave modulations [45]. Notably, the opposite trend is observed during wakefulness, with higher δ and lower β predictability during sleep. This inverse relationship is consistent with previous findings [46] reporting lower δ band power and higher β band power during REM compared to non-REM sleep. Such reciprocal behavior aligns with the hypothesis that increased predictability correlates with greater spectral power in a specific frequency band [39], and may reflect underlying regulatory mechanisms governing brain activity across states of consciousness and deserves further exploration of its implications for brain-heart interactions.

B. Analysis of static and dynamic brain-heart interplay

Our analysis of coupling revealed a low strength of interaction between HRV and EEG wave amplitude during wakefulness and at shorter time-scales, suggesting a decoupling of the brain-heart axis at $\sim$ 1s. This finding is supported by the low percentage of subjects for whom the coupling exceeds the threshold of significance, aligning with previous studies [47]. Conversely, this decoupling disappeared at longer time-scales during sleep, where significant static and dynamic coupling emerged. These findings are consistent with previous research showing strong bidirectional interactions between the cardiac vagal component and EEG rhythms at $\sim$ 1min time-scale [12], [13], [32], probably modulated by physiological transitions across different sleep stages [12].

The presence of lagged interactions across brain and heart is confirmed at longer time-scale by the higher number of subjects showing the presence of statistically significant MIR compared to MI even if with lower values. Theoretically, MIR accounts for the entire history of interactions and for this reason it should be higher than or at least equal to MI, which only captures zero-lag dependencies. The opposite trends observed can be ascribed to the difficulty of reliably estimating entropies for variables of high dimension (parameter *m*) due to the increasing sparsity of data represented in spaces of growing dimension [48]. This occurs when we move from MI to MIR estimation, and therefore the strength of the latter tends to decrease toward zero, although its presence tends to increase as the surrogate analysis showed.

We found a pivotal role of β oscillations in sustaining brain-heart interactions, as evidenced by their highest statistical significance values of coupling at longer time scales (Figs.4*d*-5*d*). This finding corroborates previous studies on the same dataset supporting the role of β waves in facilitating informa-

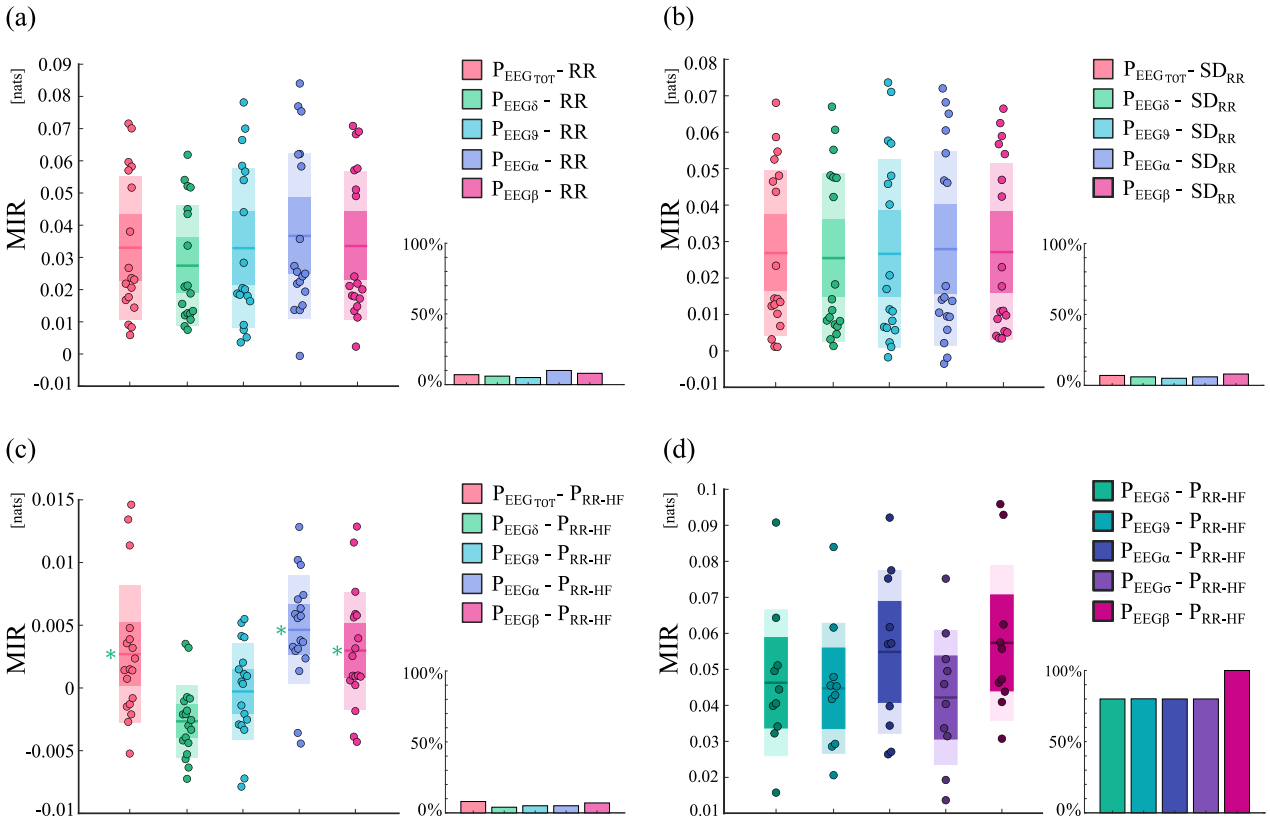

Fig. 5. Boxplots reporting the distributions and individual values of MIR computed at shorter time-scale ($\sim$ 1s) during wakefulness (panels *a-c*) and at longer time-scale ($\sim$ 1min) during sleep (panel *d*) between the cardiac *RR*, SD_{RR}, P_{RR-HF} time series and each EEG time series; the bar plots in the bottom-right part of each panel represent the percentage of subjects for whom the presence of MIR was deemed as statistically significant. For Dataset-1 (panels *a-c*, faster time-scale $\sim$ 1s), both MIR values and the percentage of MIR values identified as statistically significant, according with surrogate data analysis, were averaged across all EEG channels. Statistical test: $*$, $p < 0.05/10$, paired samples Wilcoxon test between pairs of brain rhythms, with Bonferroni correction.

tion transfer between brain and heart, as shown through linear [13] and nonlinear [12] estimators.

C. Translational Relevance

Similar methodologies have been applied in clinical research, including the study of sleep apnea-hypopnea syndrome [49] and of central-autonomic network dysregulation in paranoid schizophrenia [11], [50]. Such applications highlight the translational potential of brain-heart interaction analysis for diagnosing and treating diverse conditions [17], with biomarker identification enabling personalized interventions based on individual pathophysiological profiles.

V. Conclusions

Our findings suggest that coupling and internal dynamics are time-scale dependent, demonstrating that the dynamics of a system can be shaped by its internal processes as well as its interactions with another system. These findings align with network physiology principles, highlighting how neuro-autonomic feedback mechanisms linking brain and heart vary with temporal resolution and physiological states. Our study is limited by the inability to explore time-scale effects within the same physiological state, such as analyzing both short and long time scales during resting wakefulness. This constraint arises from the practical challenges of obtaining extended resting-state recordings and the physiological necessity of using longer time scales to study sleep transitions. These limitations highlight the need for future research to investigate brain-heart interactions across varying time scales within consistent physiological conditions, which could further refine our understanding of these complex dynamics.

References

[1] D. Azzalini, I. Rebollo, and C. Tallon-Baudry, "Visceral signals shape brain dynamics and cognition," *Trends in cognitive sciences*, vol. 23, no. 6, pp. 488–509, 2019.

[2] S. Pyner, "The paraventricular nucleus and heart failure," *Experimental physiology*, vol. 99, no. 2, pp. 332–339, 2014.

[3] P. C. Ivanov, "The new field of network physiology: building the human physiolome," *Frontiers in Network Physiology*, vol. 1, p. 711778, 2021.

[4] X. Zhao, Y. Sun, X. Li, and P. Shang, "Multiscale transfer entropy: Measuring information transfer on multiple time scales," *Communications in Nonlinear Science and Numerical Simulation*, vol. 62, pp. 202–212, 2018.

[5] G. Valenza, A. Greco, C. Gentili, A. Lanata, L. Sebastiani, D. Menicucci, A. Gemignani, and E. Scilingo, "Combining electroencephalographic activity and instantaneous heart rate for assessing brain–heart dynamics during visual emotional elicitation in healthy subjects," *Philosophical Transactions of the Royal Society A: Mathematical, Physical and Engineering Sciences*, vol. 374, no. 2067, p. 20150176, 2016.

[6] A. Zaccaro, F. Della Penna, E. Mussini, E. Parrotta, M. G. Perrucci, M. Costantini, and F. Ferri, "Attention to cardiac sensations enhances the heartbeat-evoked potential during exhalation," *Iscience*, vol. 27, no. 4, 2024.

[7] A. Bashan, R. P. Bartsch, J. W. Kantelhardt, S. Havlin, and P. C. Ivanov, "Network physiology reveals relations between network topology and physiological function," *Nature communications*, vol. 3, no. 1, p. 702, 2012.

[8] V. R. Vergara, C. Bara, R. Pernice, A. Zaccaro, F. Ferri, L. Faes, and Y. Antonacci, "Exploring the predictability of eeg signals timed with the heartbeat: A model-based approach for the temporal and spatial characterization of the brain dynamics," in *Mediterranean Conference on Medical and Biological Engineering and Computing*. Springer, 2023, pp. 135–144.

[9] Y. Antonacci, C. Barà, G. de Felice, A. Sferlazza, R. Pernice, and L. Faes, "Exploring transient neurophysiological states through local and time-varying measures of information dynamics," *Applied Mathematics and Computation*, vol. 500, p. 129437, 2025.

[10] D. Candia-Rivera, V. Catrambone, J. F. Thayer, C. Gentili, and G. Valenza, "Cardiac sympathetic-vagal activity initiates a functional brain–body response to emotional arousal," *Proceedings of the National Academy of Sciences*, vol. 119, no. 21, p. e2119599119, 2022.

[11] S. Schulz, M. Bolz, K.-J. Bär, and A. Voss, "Central-and autonomic nervous system coupling in schizophrenia," *Philosophical Transactions of the Royal Society A: Mathematical, Physical and Engineering Sciences*, vol. 374, no. 2067, p. 20150178, 2016.

[12] L. Faes, G. Nollo, F. Jurysta, and D. Marinazzo, "Information dynamics of brain–heart physiological networks during sleep," *New Journal of Physics*, vol. 16, no. 10, p. 105005, 2014.

[13] L. Faes, D. Marinazzo, F. Jurysta, and G. Nollo, "Linear and non-linear brain–heart and brain–brain interactions during sleep," *Physiological measurement*, vol. 36, no. 4, p. 683, 2015.

[14] C. J. Stam and B. W. Van Dijk, "Synchronization likelihood: an unbiased measure of generalized synchronization in multivariate data sets," *Physica D: Nonlinear Phenomena*, vol. 163, no. 3-4, pp. 236–251, 2002.

[15] K. Schiecke, B. Pester, D. Piper, F. Benninger, M. Feucht, L. Leistritz, and H. Witte, "Nonlinear directed interactions between hrv and eeg activity in children with tle," *IEEE Transactions on Biomedical Engineering*, vol. 63, no. 12, pp. 2497–2504, 2016.

[16] Y. Antonacci, C. Barà, A. Zaccaro, F. Ferri, R. Pernice, and L. Faes, "Time-varying information measures: an adaptive estimation of information storage with application to brain-heart interactions," *Frontiers in Network Physiology*, vol. 3, 2023.

[17] D. Candia-Rivera, L. Faes, F. D. V. Fallani, and M. Chavez, "Measures and models of brain-heart interactions," *arXiv preprint arXiv:2409.15835*, 2024.

[18] W. Xiong, L. Faes, and P. C. Ivanov, "Entropy measures, entropy estimators, and their performance in quantifying complex dynamics: Effects of artifacts, nonstationarity, and long-range correlations," *Physical review E*, vol. 95, no. 6, p. 062114, 2017.

[19] J. T. Lizier, *The local information dynamics of distributed computation in complex systems*. Springer Science & Business Media, 2012.

[20] A. Kraskov, H. Stögbauer, and P. Grassberger, "Estimating mutual information," *Phys. Rev. E*, vol. 69, p. 066138, Jun 2004. [Online]. Available: https://link.aps.org/doi/10.1103/PhysRevE.69.066138

[21] H. Pinto, I. Lazic, Y. Antonacci, R. Pernice, D. Gu, C. Barà, L. Faes, and A. P. Rocha, "Testing dynamic correlations and nonlinearity in bivariate time series through information measures and surrogate data analysis," *Frontiers in Network Physiology*, vol. 4, p. 138, 2024.

[22] Y. Antonacci, L. Astolfi, G. Nollo, and L. Faes, "Information transfer in linear multivariate processes assessed through penalized regression techniques: validation and application to physiological networks," *Entropy*, vol. 22, no. 7, p. 732, 2020.

[23] R. Pernice, Y. Antonacci, M. Zanetti, A. Busacca, D. Marinazzo, L. Faes, and G. Nollo, "Multivariate correlation measures reveal structure and strength of brain–body physiological networks at rest and during mental stress," *Frontiers in neuroscience*, vol. 14, p. 602584, 2021.

[24] N. Sciaraffa, J. Liu, P. Aricò, G. D. Flumeri, B. M. Inguscio, G. Borghini, and F. Babiloni, "Multivariate model for cooperation: bridging social physiological compliance and hyperscanning," *Social Cognitive and Affective Neuroscience*, vol. 16, no. 1-2, pp. 193–209, 2021.

[25] A. Greco, L. Faes, V. Catrambone, R. Barbieri, E. P. Scilingo, and G. Valenza, "Lateralization of directional brain-heart information transfer during visual emotional elicitation," *American Journal of Physiology-Regulatory, Integrative and Comparative Physiology*, vol. 317, no. 1, pp. R25–R38, 2019.

[26] C. Barà, L. Sparacino, R. Pernice, Y. Antonacci, A. Porta, D. Kugiumtzis, and L. Faes, "Comparison of discretization strategies for the model-free information-theoretic assessment of short-term physiological interactions," *Chaos: An Interdisciplinary Journal of Nonlinear Science*, vol. 33, no. 3, 2023.

[27] A. Zaccaro, M. G. Perrucci, E. Parrotta, M. Costantini, and F. Ferri, "Brain-heart interactions are modulated across the respiratory cycle via interoceptive attention," *NeuroImage*, vol. 262, p. 119548, 2022.

[28] F. Shaffer and J. P. Ginsberg, "An overview of heart rate variability metrics and norms," *Frontiers in public health*, vol. 5, p. 258, 2017.

[29] V. Catrambone, A. Greco, N. Vanello, E. P. Scilingo, and G. Valenza, "Time-resolved directional brain–heart interplay measurement through synthetic data generation models," *Annals of biomedical engineering*, vol. 47, pp. 1479–1489, 2019.

[30] A. Delorme and S. Makeig, "Eeglab: an open source toolbox for analysis of single-trial eeg dynamics including independent component analysis," *Journal of neuroscience methods*, vol. 134, no. 1, pp. 9–21, 2004.

[31] Y. Antonacci, L. Minati, D. Nuzzi, G. Mijatovic, R. Pernice, D. Marinazzo, S. Stramaglia, and L. Faes, "Measuring high-order interactions in rhythmic processes through multivariate spectral information decomposition," *IEEE Access*, vol. 9, pp. 149 486–149 505, 2021.

[32] F. Jurysta, P. Van De Borne, P.-F. Migeotte, M. Dumont, J.-P. Lanquart, J.-P. Degaute, and P. Linkowski, "A study of the dynamic interactions between sleep eeg and heart rate variability in healthy young men," *Clinical neurophysiology*, vol. 114, no. 11, pp. 2146–2155, 2003.

[33] M. Malik, "Heart rate variability: Standards of measurement, physiological interpretation, and clinical use: Task force of the european society of cardiology and the north american society for pacing and electrophysiology," *Annals of Noninvasive Electrocardiology*, vol. 1, no. 2, pp. 151–181, 1996.

[34] A. A. Borbély, F. Baumann, D. Brandeis, I. Strauch, and D. Lehmann, "Sleep deprivation: effect on sleep stages and eeg power density in man," *Electroencephalography and clinical neurophysiology*, vol. 51, no. 5, pp. 483–493, 1981.

[35] L. Faes, D. Kugiumtzis, G. Nollo, F. Jurysta, and D. Marinazzo, "Estimating the decomposition of predictive information in multivariate systems," *Physical Review E*, vol. 91, no. 3, p. 032904, 2015.

[36] T. M. Cover, *Elements of information theory*. John Wiley & Sons, 1999.

[37] M. S. Baptista, R. M. Rubinger, E. R. Viana, J. C. Sartorelli, U. Parlitz, and C. Grebogi, "Mutual information rate and bounds for it," *PLoS One*, vol. 7, no. 10, p. e46745, 2012.

[38] L. Faes, G. Mijatovic, Y. Antonacci, R. Pernice, C. Barà, L. Sparacino, M. Sammartino, A. Porta, D. Marinazzo, and S. Stramaglia, "A new framework for the time-and frequency-domain assessment of high-order interactions in networks of random processes," *IEEE Transactions on Signal Processing*, vol. 70, pp. 5766–5777, 2022.

[39] Y. Antonacci, C. Barà, L. Sparacino, I. Pirovano, A. Mastropietro, G. Rizzo, and L. Faes, "Spectral information dynamics of cortical signals uncover the hierarchical organization of the human brain's motor network," *IEEE Transactions on Biomedical Engineering*, 2024.

[40] L. Faes, A. Porta, and G. Nollo, "Mutual nonlinear prediction as a tool to evaluate coupling strength and directionality in bivariate time series: comparison among different strategies based on k nearest neighbors," *Physical Review E—Statistical, Nonlinear, and Soft Matter Physics*, vol. 78, no. 2, p. 026201, 2008.

[41] E. Vanoli, P. B. Adamson, Ba-Lin, G. D. Pinna, R. Lazzara, and W. C. Orr, "Heart rate variability during specific sleep stages: a comparison of healthy subjects with patients after myocardial infarction," *Circulation*, vol. 91, no. 7, pp. 1918–1922, 1995.

[42] G. Dirlich, T. Dietl, L. Vogl, and F. Strian, "Topography and morphology of heart action-related eeg potentials," *Electroencephalography and Clinical Neurophysiology/Evoked Potentials Section*, vol. 108, no. 3, pp. 299–305, 1998.

[43] C. Barà, A. Zaccaro, Y. Antonacci, M. Dalla Riva, A. Busacca, F. Ferri, L. Faes, and R. Pernice, "Local and global measures of information storage for the assessment of heartbeat-evoked cortical responses," *Biomedical Signal Processing and Control*, vol. 86, p. 105315, 2023.

[44] S. I. Gonçalves, F. Bijma, P. J. Pouwels, M. A. Jonker, J. P. Kuijer, R. M. Heethaar, F. H. L. Da Silva, and J. C. De Munck, "Inter-subject variability of resting state brain activity explored using a data and model-driven approach in combination with eeg-fmri," in *2008 5th IEEE International Symposium on Biomedical Imaging: From Nano to Macro*. IEEE, 2008, pp. 608–611.

[45] D. Aeschbach and A. A. Borbely, "All-night dynamics of the human sleep eeg," *Journal of sleep research*, vol. 2, no. 2, pp. 70–81, 1993.

[46] E. Werth, P. Achermann, and A. BORBÉLY, "Fronto-occipital eeg power gradients in human sleep," *Journal of sleep research*, vol. 6, no. 2, pp. 102–112, 1997.

[47] V. Catrambone, D. Candia-Rivera, and G. Valenza, "Intracortical brain-heart interplay: An eeg model source study of sympathovagal changes," *Human Brain Mapping*, vol. 45, no. 6, p. e26677, 2024.

[48] C. Barà, R. Pernice, C. A. Catania, M. Hilal, A. Porta, A. Humeau-Heurtier, and L. Faes, "Comparison of entropy rate measures for the evaluation of time series complexity: Simulations and application to heart rate and respiratory variability," *Biocybernetics and Biomedical Engineering*, vol. 44, no. 2, pp. 380–392, 2024.

[49] L. Faes, D. Marinazzo, S. Stramaglia, F. Jurysta, A. Porta, and N. Giandomenico, "Predictability decomposition detects the impairment of brain–heart dynamical networks during sleep disorders and their recovery with treatment," *Philosophical Transactions of the Royal Society A: Mathematical, Physical and Engineering Sciences*, vol. 374, no. 2067, p. 20150177, 2016.

[50] S. Schulz, J. Haueisen, K.-J. Bär, and A. Voss, "Altered causal coupling pathways within the central-autonomic-network in patients suffering from schizophrenia," *Entropy*, vol. 21, no. 8, p. 733, 2019.